

Silencing lncRNA SIX3OS1 mitigates inflammation and apoptosis in post-stroke cognitive impairment *via* miR-511-3p

Junsheng Zeng^{1,*}, Fen Yang^{2,*}, Hui Xiao¹, Wei Zhao¹, Kangping Song¹, Yan Liu¹ and Te Wang¹

¹ Department of Neurology, The Affiliated Changsha Central Hospital, University of South China, Hunan, China

² Department of Science and Education, The Affiliated Changsha Central Hospital, University of South China, Hunan, China

Abstract. The present study aimed to explore the expression and molecular mechanisms of lncRNA SIX3OS1 in post-stroke cognitive impairment (PSCI). Middle cerebral artery occlusion (MCAO) and oxygen-glucose deprivation/reoxygenation (OGD/R) were applied to establish an *in vitro* and *in vivo* model of PSCI. RT-qPCR was conducted to examine the mRNA levels of SIX3OS1, miR-511-3p, and RBP4. Morris water maze test was used to evaluate spatial learning and memory ability. Cell viability and apoptosis were examined by CCK-8 and flow cytometry. The secretion level of inflammatory factors was analyzed by ELISA. DLR and RIP assay were performed to validate the target relationship. In MCAO rats and OGD/R-induced cells, SIX3OS1 and RBP4 levels were significantly elevated, while miR-511-3p was reduced. miR-511-3p targets SIX3OS1 and RBP4. Compared with the sham, the spatial learning and memory ability of MCAO rats were decreased, but the silencing of SIX3OS1 could restore them, but this restoration was partially impaired by lowering of miR-511-3p. Silencing of SIX3OS1 enhanced OGD/R-induced SH-SY5Y cell viability and inhibited apoptosis and inflammatory factor secretion, but they were both attenuated by the lowering of miR-511-3p. Silencing of SIX3OS1 can protect PSCI *via* targeting miR-511-3p to promote cell viability and inhibit apoptosis and inflammation.

Key words: PSCI — SIX3OS1 — miR-511-3p — Apoptosis — Inflammation

Introduction

Post-stroke cognitive impairment (PSCI) is a common cerebrovascular disease induced by ischemic stroke and commonly occurs 6 months after stroke with a series of symptoms from mild cognitive impairment to dementia (Han et al. 2023). The pathogenesis of PSCI is complex and has not been completely revealed, but degenerated learning and memory abilities have been considered the major outcomes of PSCI (Zhou et al. 2022). Many researchers consider PSCI to be closely associated with Alzheimer's disease, but PSCI showed a higher incidence and mortality with rapid

development. Neuron apoptosis and neuroinflammation are involved in the onset and development of PSCI, which are also associated with Alzheimer's disease-related processes (Zhang et al. 2021; Chi et al. 2023). In the clinic, the treatment of PSCI is mainly based on the therapy strategies of stroke. Several studies have been devoted to exploring novel and effective drugs, herbs, or compounds for the therapy of PSCI, but identifying specific therapeutic targets for PSCI would improve therapy efficiency and benefit patients' prognosis.

The function of non-coding RNAs (ncRNAs) in regulating human diseases has attracted special attention in the past decades. ncRNAs have been demonstrated to be involved in various biological processes, including cell differentiation, apoptosis, proliferation, and metabolism, which are closely associated with disease progression. Moreover, there have been several studies investigating the regulation of PSCI by ncRNAs. Due to the close association between PSCI and

* The first two authors contributed equally to this work.

Correspondence to: Te Wang, Department of Neurology, The Affiliated Changsha Central Hospital, University of South China, No. 161 Shaoshan South Road, Changsha 410004, Hunan, China
E-mail: 2018050821@usc.edu.cn

Alzheimer's disease, our previous work has attempted to identify dysregulated ncRNAs in both PSCI and Alzheimer's disease and screened the lncRNA SIX3OS1/miR-511-3p axis, which was revealed to mediate the cognitive dysfunction in Alzheimer's disease and attenuate oxidative stress to regulate depression-like behaviors (Zou et al. 2020; Jia et al. 2022). Both SIX3OS1 and miR-511-3p were demonstrated to screen PSCI and predict severe disease development in our previous work. However, the mechanisms underlying the function and the interaction of SIX3OS1 and miR-511-3p have not been disclosed. Hence, further investigation was performed in the present study with the employment of rat and cell models.

This study established the PSCI rat model through the middle cerebral artery occlusion (MCAO) method, and cell models were constructed with a human neuroblastoma cell line, SH-SY5Y treated by the oxygen-glucose deprivation (OGD) method. The regulation of cognitive function of rats and cell injury by the SIX3OS1/miR-511-3p axis was investigated.

Materials and Methods

Animals and modeling

The study has obtained approval from the Ethics Committee of The Affiliated Changsha Central Hospital, University of South China. Male Sprague-Dawley rats aged 7–8 weeks and weighted 265 ± 15 g were maintained at $20 \pm 3^\circ\text{C}$ with relative humidity of 50–65%. Rats were free to drink and food for 1 week to adapt to the environment and then were randomly divided into CK and PSCI groups.

PSCI rat models were established by the MCAO method. Specifically, rats were anesthetized with 10% chloral hydrate, and then the right common carotid artery (CCA), external carotid artery (ECA), and internal carotid artery (ICA) were exposed after disinfection of the neck skin. CCA and ICA were ligatured and tied the knot near the ICA fork. A "V" shaped incision was cut at the distal end of the CCA, and the 4-0 nylon fishing line coated with polylysine was sewn into the ICA through the incision. The suture depth was 18–20 mm enough to block the blood flow at the beginning of the middle cerebral artery (MCA). The occlusion was continued for 2 h, and the plug was gently pull back to the common carotid bifurcation. The sham group, which was similar to the model group, was established without occlusion of the MCA.

Grouping of experimental animals

The rat was divided into two cohorts. The initial cohorts were utilized to investigate the function of SIX3OS1 in

PSCI. SD rats were randomly allocated into sham, MCAO, NC (MCAO + small interfering RNA (si)-negative control), and si-SIX3OS1 (MCAO + small interfering RNA targeting SIX3OS1) group ($n = 12$ per group). The second cohorts of rats were utilized to investigate the combined effects of miR-511-3p and SIX3OS1. Rats were randomly divided into the following groups: MCAO, MCAO+si-NC, MCAO+si-SIX3OS1, MCAO+si-SIX3OS1+agomir NC, and MCAO+si-SIX3OS1+miR-511-3p agomir ($n = 12$ per group). si-NC and si-SIX3OS1 were obtained from GenePharma. miR-511-3p agomir and negative control agomir NC (5 ml of 100 mM) were purchased from RIBO bio.

Intracerebroventricular injection

According to previous studies (Leem et al. 2023), rats were anesthetized and subjected to intracerebroventricular injection through a stereotactic apparatus, three days prior to the establishment of the MCAO model. The coordinates for injection were set as 1 mm posterior to the anterior fontanelle, 2.5 mm lateral to the midline, and with an insertion depth of 3.5 mm. Interfering RNA or oligonucleotide was injected into the right lateral ventricle at a flow rate of $1 \mu\text{l}/\text{min}$ for 5 min.

Modified neurologic severity scores (mNSS)

Neurologic deficits were quantified by mNSS methods based on previous studies performed by researchers blinded to the experimental subgroups. Postoperatively, and at 1, 3, and 5 days postoperatively the rats were tested for motor (muscle status and abnormal movements), sensory (visual, tactile, and proprioceptive), and reflex responses, as well as balance tests. Scores range from 0 to 18, where higher scores indicate more severe nerve damage.

Morris water maze test

The experiment employed a pool with a diameter of 160 cm and a depth of 55 cm. The pool was divided into four quadrants by the equidistant points on the wall of the pool. The depth of water was 30 cm, and the temperature was set at $24 \pm 2^\circ\text{C}$. A platform with a diameter of 12 cm and a height of 28 cm was placed in either quadrant, and the Morris water maze test included two parts: a positioning navigation experiment evaluating the learning ability and a space exploration experiment assessing the memory ability.

Serum and hippocampal tissue acquisition

After completion of behavioral testing, rats were anesthetized intraperitoneally with 10% chloral hydrate. 4–5 ml of blood

was obtained from the abdominal aorta. The upper serum was collected after centrifugation. Rats were over-anesthetized and euthanized with cervical dislocations. Rats were rapidly decapitated and de-brained, and rat hippocampal tissue was isolated and stored at -80°C .

Cell line and oxygen-glucose deprivation (OGD) treatments

SH-SY5Y cell line was purchased from ATCC (USA) incubated with DMEM culture medium reaching the logarithmic growth phase, and then the culture medium was replaced with glucose-free DMEM culture medium. The cell culture was performed at an anaerobic condition with 5% CO_2 and 95% N_2 for 4 h (OGD) and then moved to an aerobic condition (5% CO_2 and 95% O_2) incubating for another 6, 12, and 24 h (OGD/R) to establish PSCI cell model.

Cells were transfected with shRNA of SIX3OS1, miR-511-3p inhibitor, or negative controls after hypoxia-reoxygenate treatment at room temperature using Lipofectamine 3000. Transfected cells were incubated at 37°C for 48 h and then were available for the following experiments.

Real-time quantitative PCR

Total RNA is extracted from serum or cells using TRIzol reagent and subsequently assayed for purity and concentration using a NanoDrop 1000 spectrophotometer. Reverse transcription of 1.0 μg RNA for cDNA using the InRcute lncRNA First-Strand cDNA kit (cat#KR202, Tiangen) or the miRcute Plus miRNA First-Strand cDNA kit (cat#KR201, Tiangen). miRcute Plus miRNA qPCR kit (cat#FP411, Tiangen) or InRcute lncRNA qPCR kit (cat#FP402, Tiangen) was mixed with primers, cDNA, and ddH_2O for PCR amplification. GAPDH (forward 5'-AGGTCGGTGTGAACGGATTTG-3', reverse 5'-TGTAGACCATGTAGTTGAGGTCA-3') and U6 (forward 5'-GCTTCGGCAGCACATATACTAAAAT-3', reverse 5'-CGCTTCACGAATTTGCGTGTTCAT-3') were taken as internal reference genes for SIX3OS1 (forward 5'-TGTAGCAGCGGCGGATAAAT-3', reverse 5'-AGGCTTCCCAACAGGTTAGC-3') and miR-511-3p (forward 5'-GCAGAAATGTGTAGCAAAAGACA-3', reverse 5'-GGTCCAGTTTTTTTTTTTTTTTATCCT-3'). The PCR amplification was performed with the following conditions: 95°C for 6 min, followed by 25 cycles of 95°C for 30 s, 55°C for 30 s, and 72°C for 30 s, final extension at 72°C for 10 min. Relative expression of RNA was examined by $2^{-\Delta\Delta\text{Ct}}$ methods.

Cell viability

OGD/R and transfected cells were inoculated into 96-well plates. After 24 h of incubation, the cell counting kit (CCK)-8 buffer was mixed with DMEM in a ratio of 1:9 and added to

96-well plates. Subsequently, the OD value at 490 nm was measured in an enzyme labeler.

Enzyme-linked immunosorbent assay (ELISA)

The concentration of tumor necrosis factor α (TNF- α) (cat#29-8321-65, Thermo Fisher Scientific, USA), interleukin 6 (IL-6) (cat# 29-8061-65, Thermo Fisher Scientific, USA), IL-1 β (cat#29-8012-65, Thermo Fisher Scientific, USA), and IL-10 (cat#88-7105-76, Thermo Fisher Scientific, USA) in serum and cell supernatants were measured according to the instructions of the commercially available ELISA kits. Absorbance at 450 nm was determined using a Multiskan microplate reader.

Flow cytometry assay

Annexin V-fluorescein isothiocyanate/propidium iodide (FITC/PI) kit (BestBio, China) was conducted to examine the cell apoptosis. Cells after transfection and OGD/R induced were subjected to EDTA-free trypsin digestion, centrifuged, and resuspended in binding buffer. Subsequently, 5 μl of Annexin V-FITC and 5 μl of PI were dropped and incubated in the dark for 15 min, followed by the detection of apoptosis on a flow cytometer (Beckman Coulter, China).

Subcellular fractionation assay

The nuclear and cytoplasmic extracts from SH-SY5Y were isolated by PARIS kits. RNA was isolated and extracted, then the expression of U6, GAPDH, and SIX3OS1 was examined by RT-qPCR. U6 was the nuclear control and GAPDH was the cytoplasmic control.

Bioinformatics analysis

The Starbase database predicted the target miRNA of SIX3OS1, which identified miR-511-3p. Database of TargetScan, miRDB, and EvmiRNA was used to predict the targets of miR-511-3p, including RBP4.

Dual-luciferase assay and RNA-binding protein immunoprecipitation (RIP) assay

The sequences of SIX3OS1 or RBP4 containing miR-511-3p binding sites were subcloned into dual luciferase reporter plasmids (Promega, USA) to construct wild type recombinant luciferase reporter plasmids SIX3OS1-WT or RBP4-WT, and the mutation sequences of the binding sites were inserted into the plasmids to construct mutant luciferase reporter plasmids SIX3OS1-MT or RBP4-MT. SH-SY5Y cells (ATCC, USA) incubated as above described were

inoculated into 24-well plates, and the above recombinant plasmids were mixed with miR-511-3p mimic, miR-511-3p inhibitor, mimic NC, or inhibitor NC, respectively, and transfected under Lipofectamine 3000. After 48 h, the luciferase activity was detected by dual luciferase reporter assay.

The RIP assay in SH-SY5Y was conducted using the EZMagna RIP kit. The cells were lysed and then hatched with human anti-Ago 2 or negative control anti-IgG-conjugated magnetic beads. The level of RNA enriched by RIP was examined by RT-qPCR.

Statistical methods

The data were processed using the statistical software SPSS 21.0 and GraphPad prism 9.0. The data were presented as mean \pm SD, and analyzed using the independent Student's *t*-test for two-group comparisons, as well as one-way ANOVA followed by Tukey *post hoc* tests for multiple-group comparisons. Values of $p < 0.05$ were considered statistically significant.

Results

Silencing of lncRNA SIX3OS1 improves cognitive dysfunction and inflammatory injury in rats with PSCI

To investigate the functions of SIX3OS1 in PSCI, SIX3OS1 levels were modulated by lateral ventricle injection. As shown in Figure 1A, MCAO significantly increased the mRNA levels of SIX3OS1 in rats compared with the sham, but this increase was effectively inhibited by si-SIX3OS1 ($p < 0.05$). In addition, the mNSS score of MCAO rats significantly increased after MCAO surgery, and rats with silencing SIX3OS1 showed a lower mNSS score ($p < 0.05$, Fig. 1B). With the prolonged training duration, the latency to find the platform and the swimming distance were noticeably prolonged in MCAO rats than in sham; however, they were both partially reversed by silencing of SIX3OS1 ($p < 0.05$, Fig. 1C,D). Furthermore, MCAO rats had a delayed latency to find the platform, a significantly reduced number of traversals across the platform, and a decreased time spent in the target quadrant, but they were all notably reversed by silencing of SIX3OS1

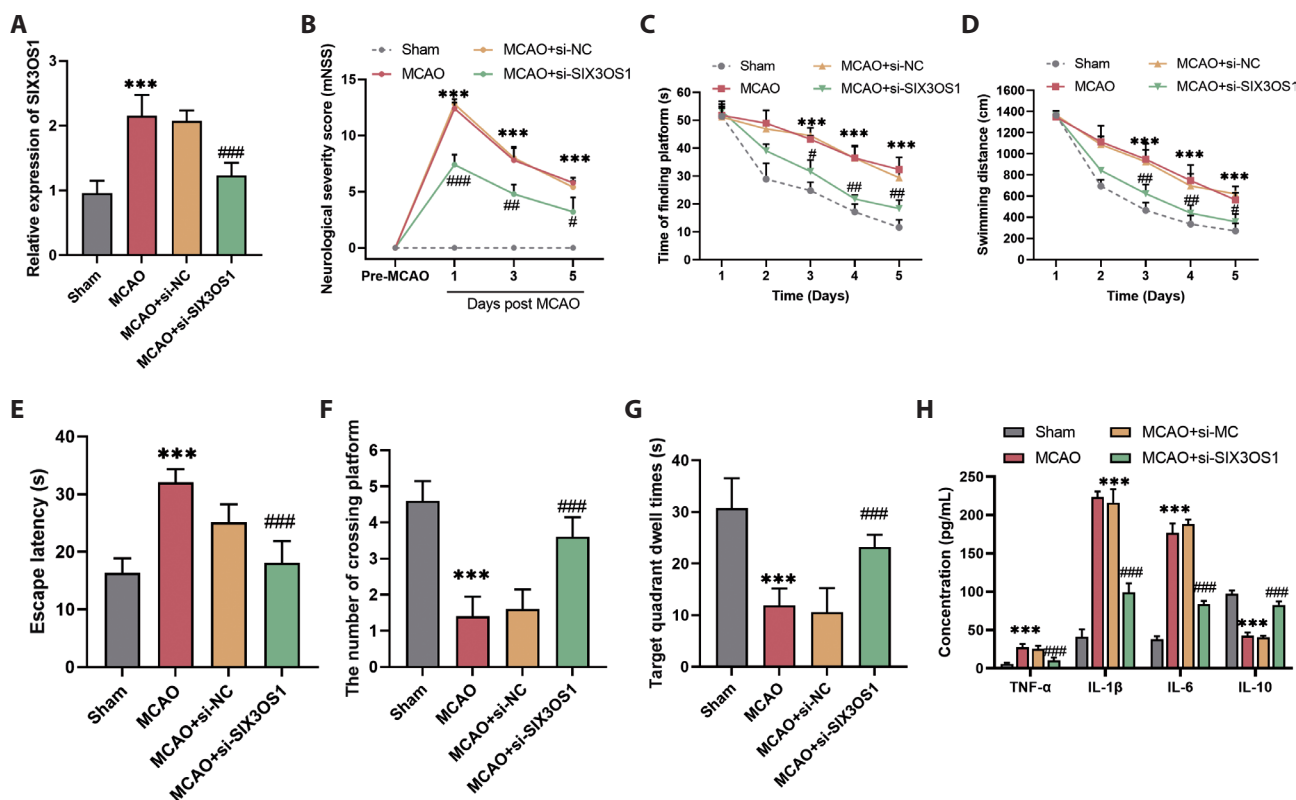


Figure 1. Silencing of lncRNA SIX3OS1 improves cognitive dysfunction and inflammatory injury in rats with PSCI. **A.** The mRNA levels of SIX3OS1 in the MCAO rats. **B.** mNSS was used to evaluate neurological deficits in rats. Morris water maze test was conducted to examine spatial learning and memory abilities in rats *via* time to find the platform (**C**), distance swum (**D**), escape latency (**E**), number of times crossing the platform (**F**), and time spent in the target quadrant (**G**). **H.** Enzyme-linked immunosorbent assay for the detection of serum inflammatory factor secretion in rats. *** $p < 0.001$ vs. Sham; # $p < 0.05$, ## $p < 0.01$, ### $p < 0.001$ vs. MCAO+si-NC.

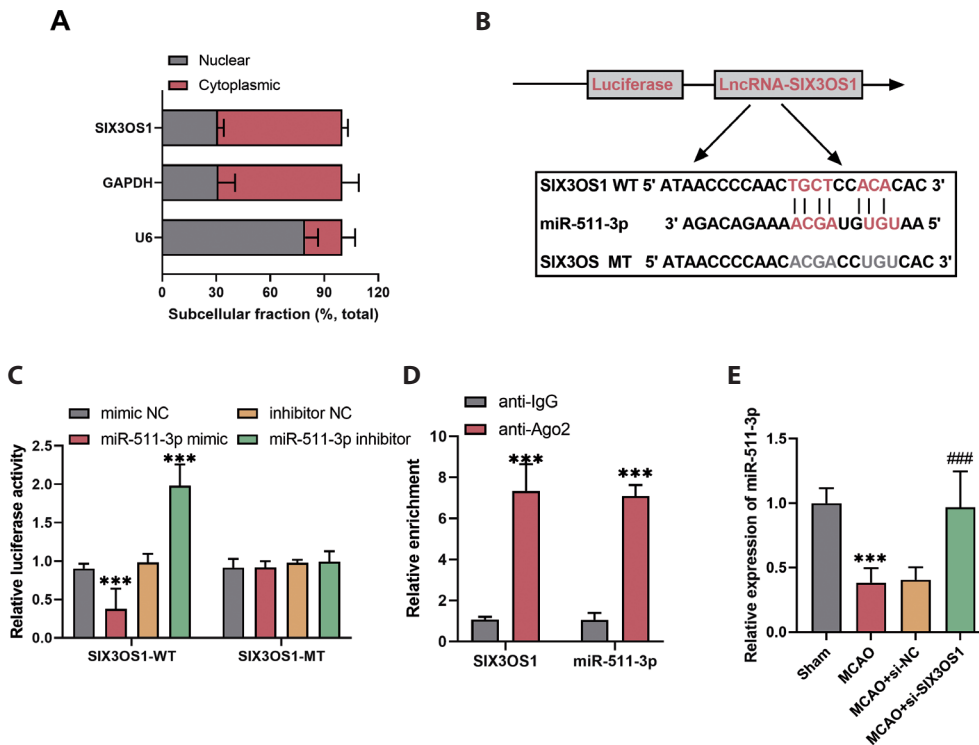


Figure 2. SIX3OS1 target miR-511-3p. **A.** SIX3OS1 expression in the cytoplasmic fraction and nucleus fraction. **B.** The binding sequence of SIX3OS1 and miR-511-3p. **C.** Dual-luciferase report assay was conducted on the target relationship between SIX3OS1 and miR-511-3p. **D.** The enrichment of miR-511-3p and SIX3OS1 in anti-Ago2 and anti-IgG was examined by RIP assay. **E.** The mRNA levels of miR-511-3p in the MCAO rats. *** $p < 0.001$ vs. Sham, mimic NC, inhibitor NC or anti-IgG; ### $p < 0.001$ vs. MCAO+si-NC. (For color figure see online version of the article.)

(Fig. 1E–G). The serum levels of pro-inflammatory factors TNF- α , IL-1 β , and IL-6 were markedly increased in MCAO rats compared with the sham, whereas the levels of the anti-inflammatory factor IL-10 were decreased, but the silencing of SIX3OS1 reversed them ($p < 0.05$, Fig. 1H).

Correlation between SIX3OS1 and miR-511-3p

lncRNAs in the cytoplasm can function as miRNA molecular sponges. SIX3OS1 was found to have higher expression in the cytoplasmic fraction compared to the nucleus ($p < 0.05$, Fig. 2A). The putative target miRNA of SIX3OS1 was predicted using a database, and a binding sequence between SIX3OS1 and miR-511-3p was identified ($p < 0.05$, Fig. 2B). In addition, high expression of miR-511-3p significantly suppressed the luciferase activity of SIX3OS1-WT but did not affect the luciferase activity of SIX3OS1-MT ($p > 0.05$, Fig. 2C). Compared with IgG, Ago2 combined with SIX3OS1 and miR-511-3p was typically increased ($p < 0.05$, Fig. 2D). Furthermore, MCAO decreased miR-511-3p expression in rat serum but silencing of SIX3OS1 significantly increased miR-511-p levels ($p < 0.05$, Fig. 2E).

SIX3OS1 acts on cognitive dysfunction and inflammatory damage in rats by targeting miR-511-3p

To further emphasize the relationship between miR-511-3p and SIX3OS1 in PSCI, miR-511-3p and SIX3OS1 were co-regulated

in MCAO rats. As shown in Figure 3A, silencing of SIX3OS1 increased miR-511-3p levels in rat serum but was effectively inhibited by miR-511-3p antagonist ($p < 0.05$). The suppression of rat mNSS scores by silencing SIX3OS1 was also partially reversed by miR-511-3p antagonist ($p < 0.05$, Fig. 3B). The shortened platform-finding latency and swimming distance of MCAO rats with SIX3OS1 silencing were noticeably reversed by lowering miR-511-3p ($p < 0.05$, Fig. 3C,D). Furthermore, the shortened platform latency, increased number of traversals across the platform, and increased target quadrant dwell time in MCAO rats by silencing of SIX3OS1 were partially diminished by low expression of miR-511-3p ($p < 0.05$, Fig. 3E–G). Silencing of SIX3OS1 suppressed TNF- α , IL-1 β , and IL-6 secretion and promoted IL-10 secretion in MCAO rats, but both were partially eliminated by miR-511-3p ($p < 0.05$, Fig. 3H).

Silencing of SIX3OS1 regulates OGD/R-induced cell viability, apoptosis, and inflammation

To further verify the involvement of SIX3OS1 in PSCI, an *in vitro* cell model was constructed by OGD/R treatment. With the time of reoxygenation after OGD, the cell viability of SH-SY5Y gradually decreased, while the expression of SIX3OS1 gradually enhanced ($p < 0.05$, Fig. 4A,B). The reoxygenation for 24 h was selected for follow-up experiments based on previous studies. Transfection of si-SIX3OS1 significantly reduced the levels of OGD/R-promoted SIX3OS1 ($p < 0.05$, Fig. 4C). Moreover, the inhibition of OGD/R on cell viability

was prominently prompted by the silencing of SIX3OS1 ($p < 0.05$, Fig. 4D). Low expression of SIX3OS1 also impaired the promotion of apoptosis by OGD/R ($p < 0.05$, Fig. 4E). Additionally, OGD/R promoted the secretion of the inflammatory factors TNF- α , IL-1 β , and IL-6, but inhibited IL-10; however, they were all partially eliminated by silencing SIX3OS1 ($p < 0.05$, Fig. 4F).

SIX3OS1 participates in OGD/R cell injury by targeting miR-511-3p

With the delay of reoxygenation time after OGD, the mRNA levels of miR-511-3p gradually decreased ($p < 0.05$, Fig. 5A). However, the promotion of miR-511-3p level by si-SIX3OS1 could

be significantly alleviated with the transfected of miR-511-3p inhibitor ($p < 0.05$, Fig. 5B). Silencing of SIX3OS1 could alleviate the inhibitory effect of OGD/R on cell viability and promote cell apoptosis, but this function was partially abolished by low expression of miR-511-3p ($p < 0.05$, Fig. 5C,D). Moreover, the inflammatory factors TNF- α , IL-1 β , and IL-6 were significantly suppressed by si-SIX3OS1 and IL-10 was promoted, which was reversed by miR-511-3p inhibitor ($p < 0.05$, Fig. 5E).

miR-511-3p targets RBP4

Bioinformatics databases predicted targets of miR-511-3p, where binding sites to RBP4 were identified, and the binding sequences were listed in Figure 6A. Moreover, elevated

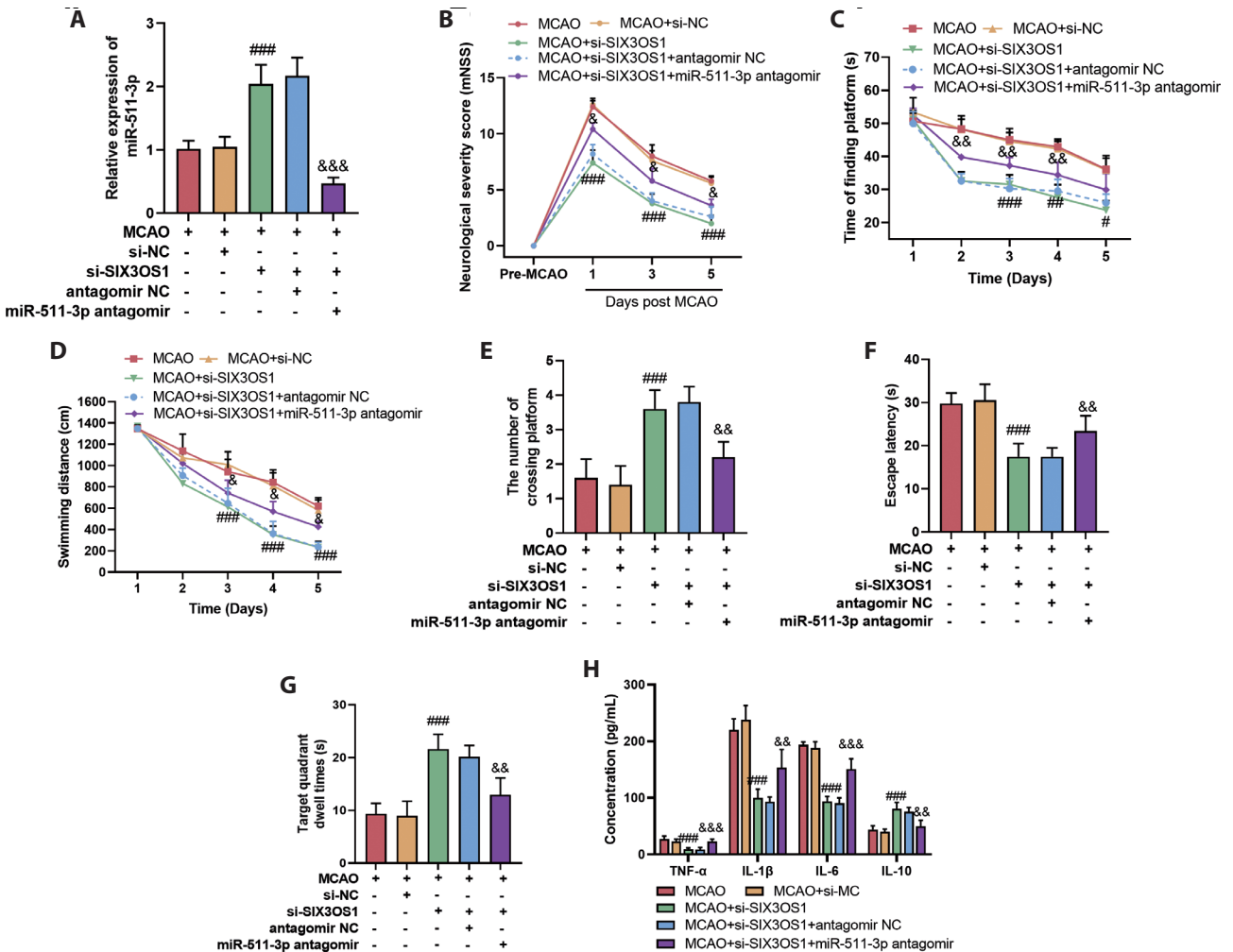


Figure 3. SIX3OS1 acts on cognitive dysfunction and inflammatory damage in rats by targeting miR-511-3p. **A.** The mRNA levels of miR-511-3p in the MCAO rats. **B.** mNSS was used to evaluate neurological deficits in rats. Morris water maze test was conducted to examine spatial learning and memory abilities in rats *via* time to find the platform (**C**), distance swum (**D**), number of times crossing the platform (**E**), escape latency (**F**), and time spent in the target quadrant (**G**). **H.** Enzyme-linked immunosorbent assay for the detection of serum inflammatory factor secretion in rats. # $p < 0.05$, ## $p < 0.01$, ### $p < 0.001$ vs. MCAO+si-NC; & $p < 0.05$, && $p < 0.01$, &&& $p < 0.001$ vs. MCAO+si-SIX3OS1+antagomir miR-511-3p.

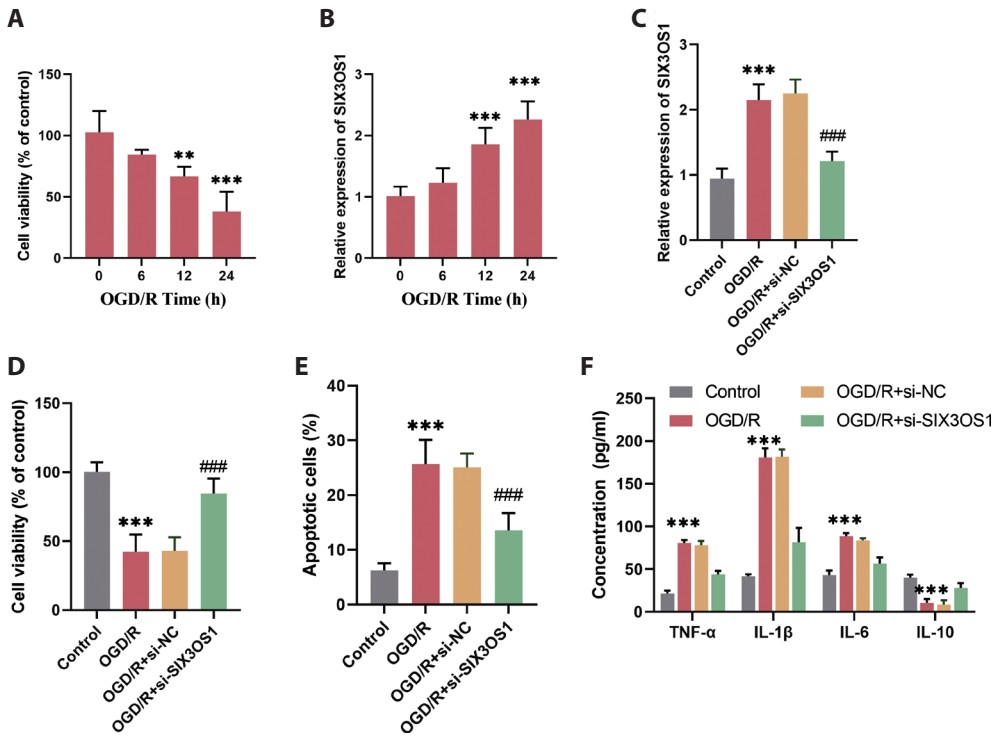


Figure 4. Effects of SIX3OS1 silencing on OGD/R induced cell viability, apoptosis, and cellular inflammation in SH-SY5Y cells. **A.** The cell viability of SH-SY5Y cells with time to reoxygenation after OGD. **B.** The mRNA levels of SIX3OS1 of SH-SY5Y cells with time to reoxygenation after OGD. **C.** SIX3OS1 levels in a cell after reoxygenation for 24 h after OGD and after transfection with si-SIX3OS1. CCK-8, flow cytometry, and ELISA assay to analyze cell viability (**D**), apoptosis (**E**), and secretion levels of inflammatory factors (**F**). ** $p < 0.01$, *** $p < 0.001$ vs. Control; ### $p < 0.001$ vs. OGD/R+si-NC.

levels of miR-511-3p suppressed the luciferase activity of RBP4-WT, decreasing miR-511-3p promoted the luciferase activity of RBP4-WT, but they had no significant effect on the luciferase activity of RBP4-MT ($p < 0.05$, Fig. 6B). Furthermore, SIX3OS1, miR-511-3p, and RBP4 were preferentially

enriched in Ago2 antibody than the IgG ($p < 0.05$, Fig. 6C). With the delay of reoxygenation time after OGD, the mRNA levels of RBP4 were gradually enhanced ($p < 0.05$, Fig. 6D). MCAO and OGD/R upregulated the expression of RBP4, whereas knockdown of SIX3OS1 suppressed its levels ($p <$

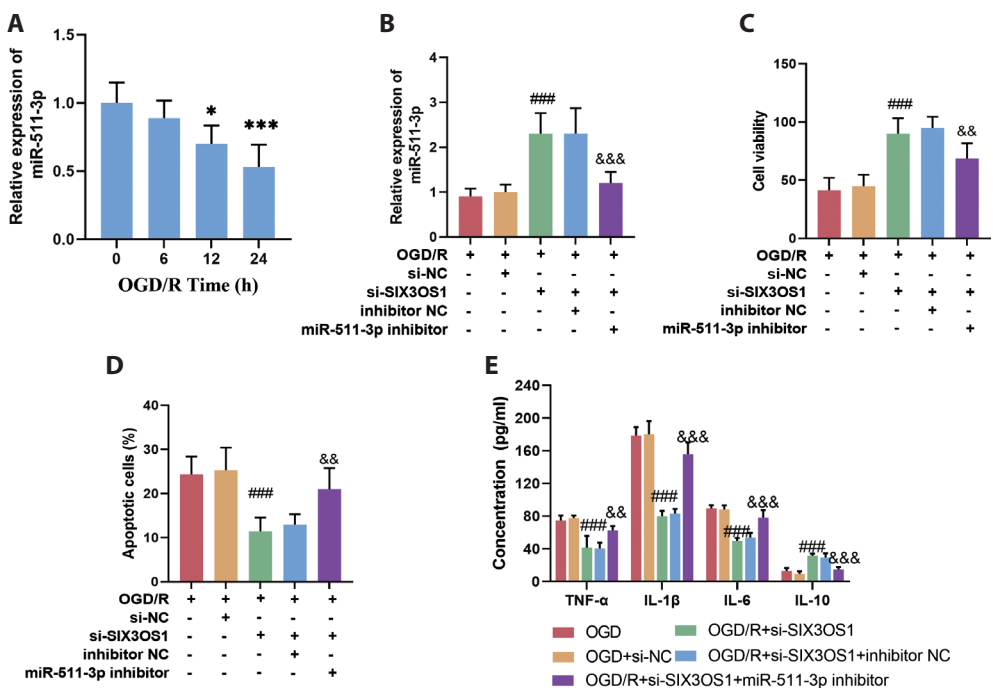


Figure 5. SIX3OS1 participates in OGD/R cell injury by targeting miR-511-3p. **A.** With the delay of reoxygenation time after OGD, the mRNA levels of miR-511 were examined. **B.** Effect of co-transfection of si-SIX3OS1 and miR-511-3p inhibitor on miR-511-3p levels in OGD/R cells. CCK-8, flow cytometry, and ELISA assay to analyze cell viability (**C**), apoptosis (**D**), and secretion levels of inflammatory factors (**E**). * $p < 0.05$, *** $p < 0.001$ vs. 0 h; ### $p < 0.001$ vs. OGD/R+si-NC; && $p < 0.01$, &&& $p < 0.001$ vs. OGD/R+si-SIX3OS1+inhibitor NC.

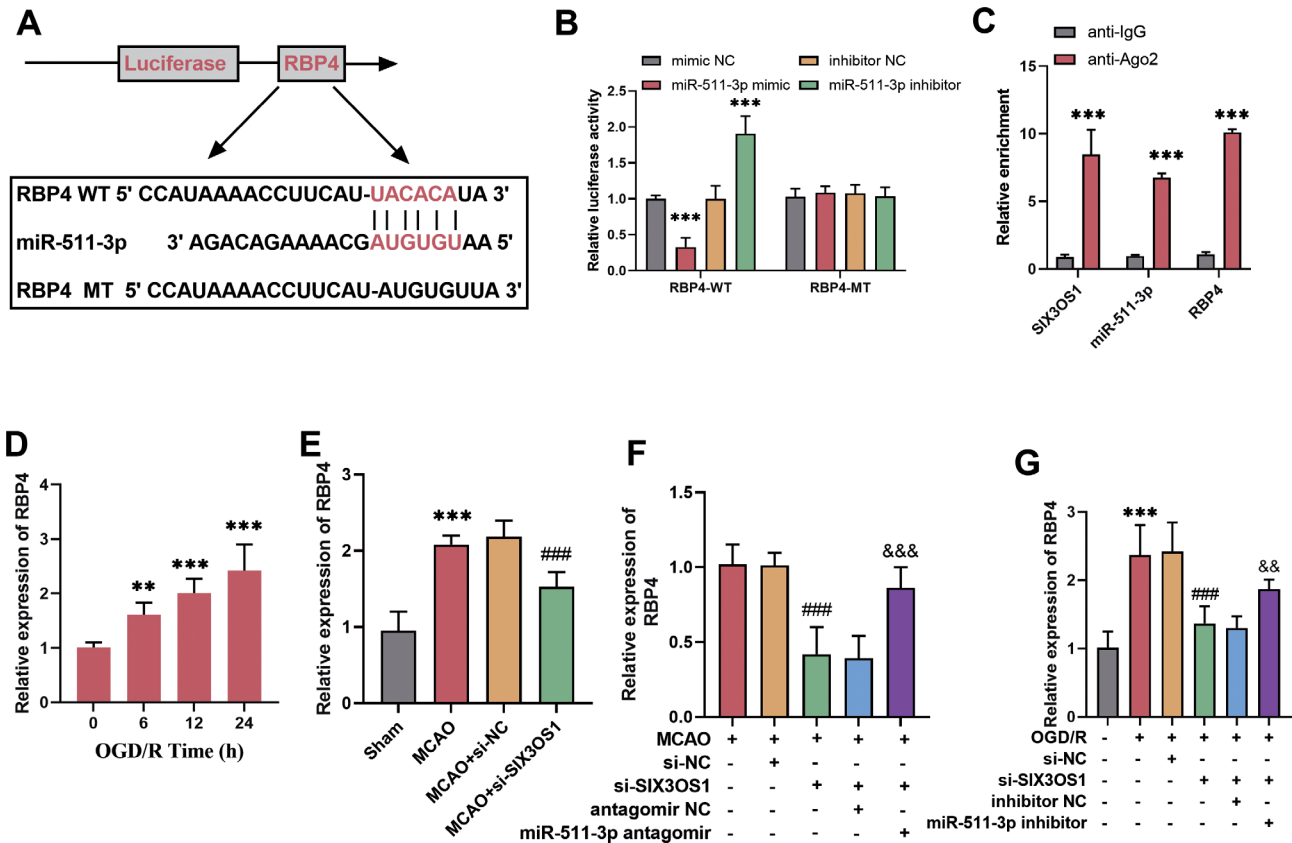


Figure 6. miR-511-3p targets RBP4. **A.** The binding sequences of RBP4 and miR-511-3p. Dual luciferase reporter assay (**B**) and RIP assay (**C**) verified the target relationship between miR-511-3p and RBP4. **D.** With the time of reoxygenation after OGD, the mRNA levels of RBP4 were determined. **E, F.** Effects of MCAO and si-SIX3OS1 or miR-511-3p antagomir on RBP4 levels in rats. **G.** Effects of OGD/R and si-SIX3OS1 or miR-511-3p inhibitor on RBP4 levels in SH-SY5Y. ** $p < 0.01$, *** $p < 0.001$ vs. mimic NC, inhibitor NC, 0 h, or sham; ### $p < 0.001$ vs. MCAO+si-NC or OGD/R+si-NC; && $p < 0.01$, &&& $p < 0.001$ vs. MCAO+si-SIX3OS1+antagomir NC or OGD/R+si-SIX3OS1+miR-511-3p inhibitor.

0.05); however, this reduction was notably attenuated by low expression of miR-511-3p ($p < 0.05$, Fig. 6E–G).

Discussion

In this preliminary research, we investigated the function of SIX3OS1 in PSCI by establishing the MCAO rat model and OGD/R-induced cell model. Our findings indicate that MCAO rats exhibit impaired spatial learning and memory functions; however, silencing of SIX3OS1 may alleviate the effects of MCAO. This may be related to the fact that silencing SIX3OS1 could restore neuronal cell viability and inhibit apoptosis and inflammatory secretion by promoting miR-511-3p.

Previous studies have disproved the function of ncRNAs in a variety of central nervous system disorders (including ischemic stroke, hemorrhagic stroke, traumatic brain injury, Alzheimer's disease, and stroke). For example, MEG3 is abnormally elevated in patients with Alzheimer's disease and is associated with necroptosis (Balusu et al. 2023). lncRNA H19

is transported from neurons to astrocytes *via* exosomes and is involved in the progression of ischemic stroke (Wang J et al. 2023). SIX3OS1, a novel lncRNA, acts as a molecular scaffold to recruit histone-modifying enzymes to the cognate structure domain factor SIX3, which plays a crucial role in the control of neural development. Pre-existing studies found that geniposide treatment ameliorated oxidative stress injury in mice with depressive behavior by promoting SIX2OS1 levels in neurons (Zou et al. 2020). In addition, geniposide ameliorated depression by transcriptional activation of SIX3OS1 upregulating the expression of synapse-associated proteins (Li et al. 2023). Patients with PSCI tend to be more likely to experience depression and have significantly higher depression scores (Zhong et al. 2021). Additionally, small vessel disease as well as Alzheimer's disease pathology collectively drive the pathogenesis of PSCI (Yoon et al. 2021). SIX3OS1 suppressed the clearance of A β 1-42 in Alzheimer's disease hippocampal tissue, increased neuronal damage, and accelerated cognitive impairment (Jia et al. 2022). Based on the above background we suspected that SIX3OS1 might be implicated in the progression of PSCI.

MCAO rat model and OGD/R-induced SH-SY5Y are widely used to study the molecular mechanisms of PSCI (Wang et al. 2020; Chi et al. 2023). In the present study, we found that the levels of SIX3OS1 were abnormally elevated in both the MCAO rats and the OGD/R-induced cells. The mNSS score as a neurological deficit score was elevated in MCAO rats, but this score could be suppressed by the silencing of SIX3OS1 (Chen et al. 2022). In addition, cognitive dysfunction with degradation of learning and memory abilities is the most common in PSCI (Sun et al. 2022). To determine the role of SIX3OS1 in cognitive dysfunction, we assessed spatial learning and memory in rats using the widely available Morris water maze test. Consistent with previous studies, spatial learning and memory abilities declined in MCAO rats (Wang G et al. 2023), however, we found for the first time that this phenomenon was improved when SIX3OS1 was suppressed. Inflammation and apoptosis are involved in the progression of PSCI (Chi et al. 2023). We found that silencing of SIX3OS1 significantly alleviated the secretion of pro-inflammatory factors and inhibited apoptosis in OGD/R-induced microglia. These results suggest that SIX3OS1 may promote the occurrence of cognitive dysfunction in PSCI by enhancing the overproduction of inflammatory factors and accelerating neuroapoptosis.

As one of numerous miRNAs, miR-511-3p has been extensively documented as a regulator of inflammatory mediators, including pulmonary inflammation induced by cockroach allergen (Do et al. 2019), asthma (Zhou et al. 2018), and meningitis (Yu et al. 2014). miR-511-3p also participates in the pathologic progression of nerve injury. For example, hypoxia preconditioned mesenchymal exosome miR-511-3p alleviates spinal cord injury (Huang et al. 2022). Interestingly, miR-511-3p levels were decreased in stroke patients and were an independent predictor of PSCI patients (Wang T et al. 2023a). Additionally, serum miR-511-3p has the potential to diagnose Alzheimer's disease and take part in the inflammatory response (Wang T et al. 2023b). Thus we suspected that miR-511-3p might also engaged in PSCI progression. Previous studies confirmed the targeting relationship between SIX3OS1 and miR-511-3p (Jia et al. 2022), which is consistent with our findings. We also found for the first time that miR-511-3p was significantly reduced in MCAO rats and OGD/R-induced cells. In addition, low expression of miR-511-3p partially attenuated the mitigating effect of silenced SIX3OS1 on PSCI and increased cell viability, inhibited apoptosis and inflammatory secretion. We demonstrated that SIX3OS1 is involved in PSCI by targeting the inhibition of miR-511-3p.

In stroke patients, RBP4 is strongly associated with disease prognosis and RBP4 predicts lesion size and severity in acute stroke (Liu and Che 2019). RBP4 is also involved in cognitive decline after stroke (Wang F et al. 2023). RBP4 is associated with neurological recovery, relapse, and death in

acute stroke (Liu et al. 2023). Furthermore, RBP4 was found to be abnormally expressed in Alzheimer's disease (Ishii et al. 2019). In our study, we found that RBP4 is a target of miR-511-3p, and MCOA and GOD/R promoted the level of RBP4, but this promotion was greatly impaired by the silencing of SIX3OS1. However, the low expression of miR-511-3p significantly restored its expression. Thus, SIX3OS1 may be engaged in PSCI by targeting the regulation of the miR-511-3p/RBP4 axis, however, this needs to be further investigated.

Our study has provided strong evidence that silencing of SIX3OS1 can promote the recovery of neurological function in PSCI by promoting miR-511-3p/RBP4 axis, inhibiting cell apoptosis and inflammation. This provides a new perspective on the treatment of PSCI patients.

Ethics approval and consent to participate. The experimental procedures were all in accordance with the guideline of the Ethics Committee of The Affiliated Changsha Central Hospital, University of South China. This study complies with the Declaration of Helsinki. A signed written informed consent was obtained from each patient.

Availability of data and materials. The data used and analyzed can be obtained from the corresponding author under a reasonable request.

Conflict of interests. The authors declare that they have no competing interests.

Funding. Scientific Research Project of Hunan Provincial Health Commission (B202303076877), and Natural Science Foundation of Hunan Province (No. 2024JJ9493).

References

- Balusu S, Horre K, Thrupp N, Craessaerts K, Snellinx A, Serneels L, T'Syen D, Chrysidou I, Arranz AM, Sierksma A, et al. (2023): MEG3 activates necroptosis in human neuron xenografts modeling Alzheimer's disease. *Science* **381**, 1176-1182
<https://doi.org/10.1126/science.abp9556>
- Chen H, Luo Y, Tsoi B, Gu B, Qi S, Shen J (2022): Angong Niu Huang Wan reduces hemorrhagic transformation and mortality in ischemic stroke rats with delayed thrombolysis: involvement of peroxynitrite-mediated MMP-9 activation. *Chin. Med.* **17**, 51
<https://doi.org/10.1186/s13020-022-00595-7>
- Chi X, Fan X, Fu G, Liu Y, Zhang Y, Shen W (2023): Research trends and hotspots of post-stroke cognitive impairment: a bibliometric analysis. *Front. Pharmacol.* **14**, 1184830
<https://doi.org/10.3389/fphar.2023.1184830>
- Chi X, Wang L, Liu H, Zhang Y, Shen W (2023): Post-stroke cognitive impairment and synaptic plasticity: A review about the mechanisms and Chinese herbal drugs strategies. *Front. Neurosci.* **17**, 1123817
<https://doi.org/10.3389/fnins.2023.1123817>
- Do DC, Mu J, Ke X, Sachdeva K, Qin Z, Wan M, Ishmael FT, Gao P (2019): miR-511-3p protects against cockroach allergen-

- induced lung inflammation by antagonizing CCL2. *JCI Insight* **4**, e126832
<https://doi.org/10.1172/jci.insight.126832>
- Han M, He J, Chen N, Gao Y, Wang Z, Wang K (2023): Intermittent theta burst stimulation vs. high-frequency repetitive transcranial magnetic stimulation for post-stroke cognitive impairment: Protocol of a pilot randomized controlled double-blind trial. *Front. Neurosci.* **17**, 1121043
<https://doi.org/10.3389/fnins.2023.1121043>
- Huang T, Jia Z, Fang L, Cheng Z, Qian J, Xiong F, Tian F, He X (2022): Extracellular vesicle-derived miR-511-3p from hypoxia preconditioned adipose mesenchymal stem cells ameliorates spinal cord injury through the TRAF6/S1P axis. *Brain Res. Bull.* **180**, 73-85
<https://doi.org/10.1016/j.brainresbull.2021.12.015>
- Ishii M, Kamel H, Iadecola C (2019): Retinol binding protein 4 levels are not altered in preclinical Alzheimer's disease and not associated with cognitive decline or incident dementia. *J. Alzheimers Dis.* **67**, 257-263
<https://doi.org/10.3233/JAD-180682>
- Jia YM, Zhu CF, She ZY, Wu MM, Wu YY, Zhou BY, Zhang N (2022): Effects on autophagy of moxibustion at governor vessel acupoints in APP/PS1 double-transgenic Alzheimer's disease mice through the lncRNA Six3os1/miR-511-3p/AKT3 molecular axis. *Evid. Based Complement. Alternat. Med.* **2022**, 3881962
<https://doi.org/10.1155/2022/3881962>
- Leem KH, Kim S, Kim HW, Park HJ (2023): Downregulation of microRNA-330-5p induces manic-like behaviors in REM sleep-deprived rats by enhancing tyrosine hydroxylase expression. *CNS Neurosci. Ther.* **29**, 1525-1536
<https://doi.org/10.1111/cns.14121>
- Li B, Zhao Y, Zhou X, Peng C, Yan X, Zou T (2023): Geniposide improves depression by promoting the expression of synapse-related proteins through the Creb1/Six3os1 axis. *Gene* **877**, 147564
<https://doi.org/10.1016/j.gene.2023.147564>
- Liu C, Che Y (2019): Retinol-binding protein 4 predicts lesion volume (determined by MRI) and severity of acute ischemic stroke. *Neurotox. Res.* **35**, 92-99
<https://doi.org/10.1007/s12640-018-9933-z>
- Liu C, Gu J, Yao Y (2023): Longitudinal change of plasma retinol-binding protein 4 and its relation to neurological-function recovery, relapse, and death in acute ischemic stroke patients. *Tohoku J. Exp. Med.* **260**, 293-300
<https://doi.org/10.1620/tjem.2023.J036>
- Sun X, Li M, Li Q, Yin H, Jiang X, Li H, Sun Z, Yang T (2022): Post-stroke cognitive impairment research progress on application of brain-computer interface. *Biomed. Res. Int.* **2022**, 9935192
<https://doi.org/10.1155/2022/9935192>
- Wang F, Qin Y, Li Z (2023): Serum retinol-binding protein 4 in stroke patients: correlation with T helper 17/regulatory T cell imbalance and 3-year cognitive function decline. *Front. Neurol.* **14**, 1217979
<https://doi.org/10.3389/fneur.2023.1217979>
- Wang G, Tang X, Zhao F, Qin X, Wang F, Yang D, Zhu H, Chen X (2023): Total saponins from *Trillium tschonoskii* Maxim promote neurological recovery in model rats with post-stroke cognitive impairment. *Front. Pharmacol.* **14**, 1255560
<https://doi.org/10.3389/fphar.2023.1255560>
- Wang J, Cao B, Gao Y, Chen YH, Feng J (2023): Exosome-transported lncRNA H19 regulates insulin-like growth factor-1 via the H19/let-7a/insulin-like growth factor-1 receptor axis in ischemic stroke. *Neural Regen. Res.* **18**, 1316-1320
<https://doi.org/10.4103/1673-5374.357901>
- Wang T, Zhao W, Liu Y, Song K, Zeng J, Wang Z (2023a): Differentially expressed miR-511-3p in stroke patients predicts the present of post-stroke cognitive impairment. *Dement Geriatr. Cogn. Disord.* **53**, 12-18
<https://doi.org/10.1159/000535631>
- Wang T, Zhao W, Liu Y, Yang D, He G, Wang Z (2023b): MicroRNA-511-3p regulates Abeta(1-40) induced decreased cell viability and serves as a candidate biomarker in Alzheimer's disease. *Exp. Gerontol.* **178**, 112195
<https://doi.org/10.1016/j.exger.2023.112195>
- Wang ZQ, Li K, Huang J, Huo TT, Lv PY (2020): MicroRNA Let-7i is a promising serum biomarker for post-stroke cognitive impairment and alleviated OGD-induced cell damage in vitro by regulating Bcl-2. *Front. Neurosci.* **14**, 215
<https://doi.org/10.3389/fnins.2020.00215>
- Yoon B, Yang DW, Hong YJ, Kim T, Na S, Noh SM, Park HL, Ku BD, Yang YS, Choi H, et al. (2021): Cognitive decline according to amyloid uptake in patients with poststroke cognitive impairment. *Medicine (Baltimore)* **100**, e27252
<https://doi.org/10.1097/MD.00000000000027252>
- Yu L, Liao Q, Zeng X, Lv Z, Zheng H, Zhao Y, Sun X, Wu Z (2014): MicroRNA expressions associated with eosinophilic meningitis caused by *Angiostrongylus cantonensis* infection in a mouse model. *Eur. J. Clin. Microbiol. Infect. Dis.* **33**, 1457-1465
<https://doi.org/10.1007/s10096-014-2087-x>
- Zhang L, Qian Y, Li J, Zhou X, Xu H, Yan J, Xiang J, Yuan X, Sun B, Sisodia SS, et al. (2021): BAD-mediated neuronal apoptosis and neuroinflammation contribute to Alzheimer's disease pathology. *iScience* **24**, 102942
<https://doi.org/10.1016/j.isci.2021.102942>
- Zhong HH, Qu JF, Xiao WM, Chen YK, Liu YL, Wu ZQ, Qiu DH, Liang WC (2021): Severity of lesions involving the cortical cholinergic pathways may be associated with cognitive impairment in subacute ischemic stroke. *Front. Neurol.* **12**, 606897
<https://doi.org/10.3389/fneur.2021.606897>
- Zhou HY, Huai YP, Jin X, Yan P, Tang XJ, Wang JY, Shi N, Niu M, Meng ZX, Wang X (2022): An enriched environment reduces hippocampal inflammatory response and improves cognitive function in a mouse model of stroke. *Neural Regen. Res.* **17**, 2497-2503
<https://doi.org/10.4103/1673-5374.338999>
- Zhou Y, Do DC, Ishmael FT, Squadrito ML, Tang HM, Tang HL, Hsu MH, Qiu L, Li C, Zhang Y, et al. (2018): Mannose receptor modulates macrophage polarization and allergic inflammation through miR-511-3p. *J. Allergy Clin. Immunol.* **141**, 350-364.e8
<https://doi.org/10.1016/j.jaci.2017.04.049>
- Zou T, Sugimoto K, Zhang J, Liu Y, Zhang Y, Liang H, Jiang Y, Wang J, Duan G, Mei C (2020): Geniposide alleviates oxidative stress of mice with depression-like behaviors by upregulating Six3os1. *Front. Cell. Dev. Biol.* **8**, 553728
<https://doi.org/10.3389/fcell.2020.553728>

Received: April 12, 2024

Final version accepted: June 21, 2024